ELSEVIER

Journal of Nuclear Materials 307–311 (2002) 1031–1036

journal of nuclear materials

www.elsevier.com/locate/jnucmat

Activation analysis of structural materials irradiated by fusion and fission neutrons

Qunying Huang [a,*], Shanliang Zheng [a], Yixue Chen [b], Jiangang Li [a]

[a] *Institute of Plasma Physics, Chinese Academy of Sciences, P.O. Box 1126, Hefei, Anhui 230031, China*
[b] *Forschungszentrum Karlsruhe, Institute for Reactor Safety, P.O. Box 3640, D-76021 Karlsruhe, Germany*

Abstract

The induced radioactivity of a few structural materials by D–T fusion neutrons and fission neutrons in a hybrid blanket have been calculated based on the fusion driven systems as the reference reactors. The neutron transport and activation calculations are done by the Monte Carlo transport code MCNP/4B and the activation inventory code FISPACT with the latest released IAEA Fusion Evaluated Nuclear Data Library (FENDL-2) and the ENDF/B-V uranium evaluated data. The effects of material types, impurities and energy spectra on the activation characteristics of materials are analyzed.

1. Introduction

Along with the ongoing efforts to utilize fusion as an energy source, there is renewed interest in fusion neutron source applications for purpose such as resource utilization and long-lived radioactive waste transmutation with fusion–fission hybrid systems [1–4]. New material technologies are needed to meet development of innovative fuel cycle and hybrid reactor technologies [5–11].

The neutron-induced activity in fusion reactor components can be effectively controlled by the proper selection of structural materials, such as those for the first wall and blanket materials, and is greatly influenced by the concentration of their composing elements. Research on low activation materials, such as vanadium alloys and ferritic steels, is being done throughout the world to ensure the attractiveness of fusion nuclear power regarding safety and environmental aspects [12–17].

The effects of neutron irradiation on structural materials in a nuclear facility mainly include two aspects: damage effects (degradation of various properties due to atomic displacement and transmutation etc.) on the materials and the impact of induced radioactivity on the environment. The induced radioactivity of the structural materials (including 316L stainless steel, ferritic steel and vanadium alloy) irradiated by D–T fusion neutrons and hybrid reactor neutrons has been studied in this paper based on the referenced neutron energy spectra in the blanket of the fusion driven systems (FDS) [1] i.e. the He gas-cooled Li_2O tritium breeding blanket (TBB) [18] and the liquid LiPb–He gas dual-cooled fuel breeding blanket (FBB) [19]. They have the same plasma core and inboard blanket, the difference between them is the outboard blanket as the names show. The following four aspects affecting the activation properties of structural materials in a fusion device or a hybrid reactor are considered: (1) neutron irradiation conditions (spectrum, strength, and irradiation time etc.); (2) types of irradiated materials; (3) impurities in the structural materials; (4) the effects of fission neutrons in the blanket on the activation characteristics of the structural materials in comparison with those with only fusion neutrons.

Two kinds of low activation materials, including vanadium alloy and ferritic steel, and their impurity effects on the activation characteristics of them when used as the blanket structural materials with D–T fusion neutron spectrum and hybrid neutron spectrum are investigated. For the purpose of comparison, the analysis of non-low activation stainless steel 316L is also included. It is assumed that they are irradiated as the first

* Corresponding author.
E-mail address: huang@mail.ipp.ac.cn (Q. Huang).

0022-3115/02/$ - see front matter
PII: S0022-3115(02)01306-5

wall and structural materials in the FDS-RT designs by 0.5 and 10 MW/m^2 neutron wall loadings under a typical neutron fluence of 15 MW year/m^2.

2. Codes, data libraries and calculation model

The neutron spectra were calculated with the Monte Carlo transport code MCNP/4B [20] and the latest data library FENDL/2.0 except uranium isotopes data from ENDF/B-V for TBB and FBB models. These spectra are inputs to the inventory code FISPACT-99 [21] using the FENDL/A-2.0 data library to calculate the activities of the structural materials based on the typical fusion and hybrid blanket arrangement. We assume the above three kinds of materials as the structural materials, respectively, and analyze the activation characteristics of them in the fusion and hybrid spectra.

The basic geometrical and material arrangements of the TBB and FBB models are the same except that three fuel material zones are included in the FBB model. The details of the TBB and FBB models can be seen in Ref. [18,19]. The activation characteristics for the three kinds of materials in the structural walls (SWs), assumed to be the third wall for the TBB model or the fifth wall for the FBB model, are calculated and analyzed.

3. Results and analysis

The activation properties and the factors affecting them have been studied for the assumed structural materials i.e. vanadium alloy VH1 (NIFS-HEAT-1 ingot), ferritic steel FS and stainless steel 316L. The compositions of these materials are from Ref. [22–24], respectively.

3.1. Neutron energy spectra

Neutron spectra of the SWs for the two models are shown in Fig. 1. It is clear that the spectra for the three kinds of structural materials have similar shapes at the SW and there are peaks at low and high neutron energies for both of the models. However, the fluxes for the FBB models have much higher values than those for the TBB models at low neutron energy, this is because of lower energy fission neutrons in the FBB. The fluxes in the SW with VH1 as the structural material are the highest compared with other two SWs with the same model.

3.2. Effects of irradiation conditions

To investigate the effects of neutron irradiation conditions, e.g. spectrum, strength and irradiation time on the activation characteristics of the materials, we analyze the activation characteristics of the SWs.

The activation levels for the TBB model under 15 MW year/m^2 are shown in Fig. 2. The dose rate of 316L is the highest among the three kinds of structural materials, dose of VH1 is the lowest when time after irradiation is less than 100 years, after that time the dose of FS is the lowest. Moreover, changing the neutron wall loading from 0.5 to 10 MW/m^2, but keeping the neutron irradiation fluence on the first wall, the doses of irradiated material have almost the same value when the time after irradiation is longer than 100 years. That is because the dominant nuclides within 100 years of time have short or medium half-lives and decay almost completely during this period of time. That means the long-term dose closely depends on the neutron fluence. The short-term dose depends on neutron source intensity i.e. neutron wall loading P_w [25].

For the TBB model, dose rates of 316L, FS and VH1 after one year's cooling are 2.98×10^3, 1.20×10^3 and

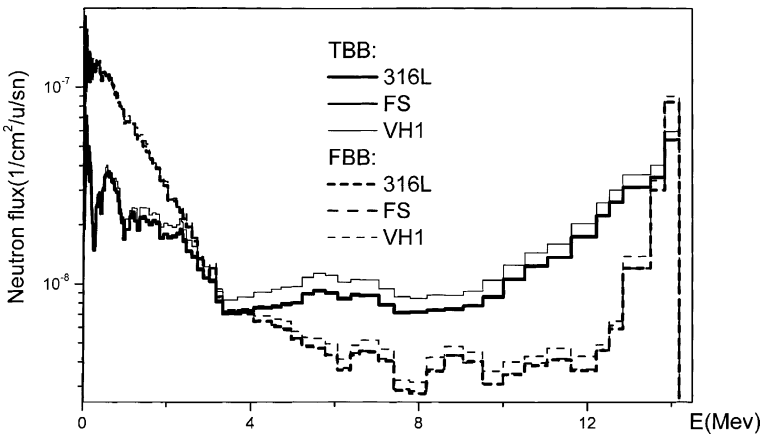

Fig. 1. Spectra of the SWs from the TBB and FBB models.

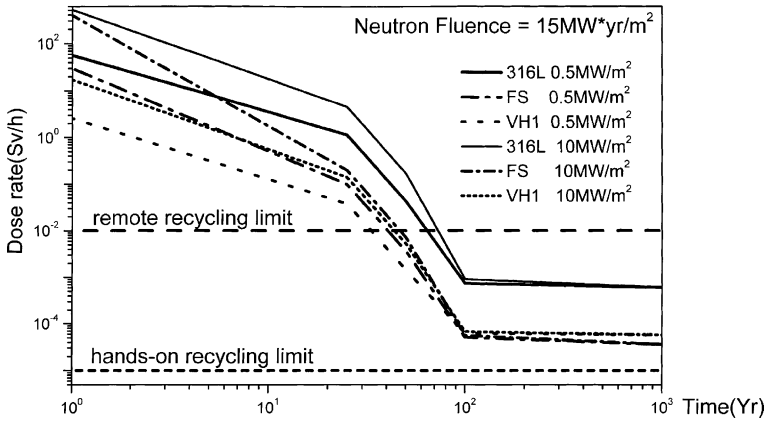

Fig. 2. Doses of the SWs from the TBB model at $P_w = 5$ and 10 MW/m^2.

18.1 Sv/h for $P_w = 0.5$ MW/m^2, and 2.56×10^4, 1.42×10^4 and 3.24×10^2 Sv/h for $P_w = 10$ MW/m^2. The dose rates for 316L, FS and VH1 are less than the remote-recycled dose rate level 0.01 mSv/h after 63, 40 or 32 years, cooling for $P_w = 0.5$ MW/m^2 and 73, 48 or 46 years cooling for $P_w = 10$ MW/m^2 based on the currently fabricated impurity level.

For the FBB model, the trend of the dose rate of the SW material varying with time after irradiation are almost the same as those for the TBB model for each of the SW materials. Fig. 3 gives the dose rates of the two models when $P_w = 0.5$ MW/m^2. The dose rate of 316L, FS or VH1 is less than the level for remote recycling after 66, 56 or 42 years' cooling.

As shown in Figs. 2 and 3, it is clear that the contact dose rates vs. time after irradiation have a similar trend for both of the models for 316L, FS and VH1, respectively, although there are some differences between dose rates of the two models. Compared with the TBB model, the total dose rate for the FBB model is two times higher for VH1, four times higher during 25–50 years' cooling time and almost the same after 100 years' cooling for FS. This is due to the different spectra from pure fusion neutrons of the TBB model and fusion hybrid neutrons of the FBB model. The dose rate of 316L, FS or VH1 is less than the remote-recycling limit for less than 100 years' cooling for $P_w = 0.5$ MW/m^2 for both blankets.

3.3. Effects of material impurities

The effect of impurities on its total activity is relatively not important because of the large amount of high activation compositions in the 316L stainless steel, therefore only the effects of impurities on the total activity level of VH1 and FS are included in the analysis.

3.3.1. Vanadium alloy VH1

The contact dose rates as a function of time after irradiation for VH1 are given in Figs. 4 and 5. It is noted that the isotope Co60 dominates the total dose

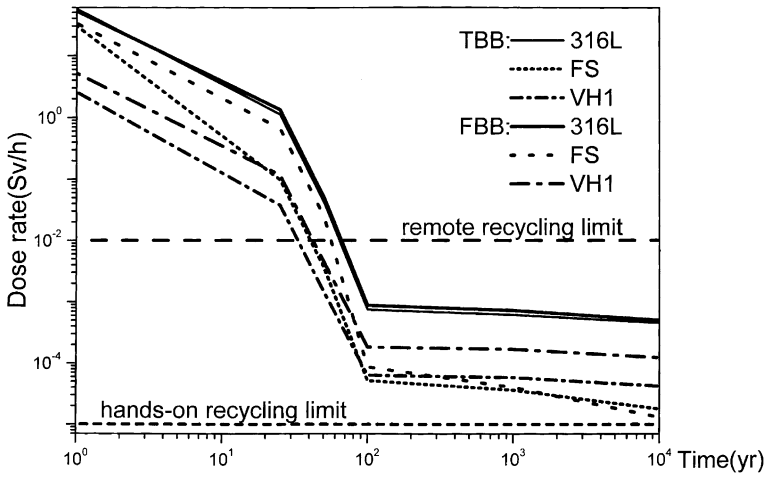

Fig. 3. Doses of the SWs after irradiation for 30 years at $P_w = 0.5$ MW/m^2.

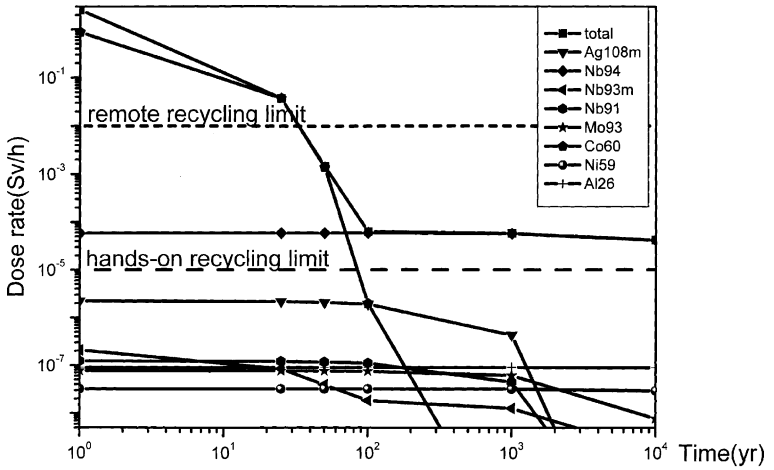

Fig. 4. Contribution of impurities to the dose rate of VH1 from the TBB model.

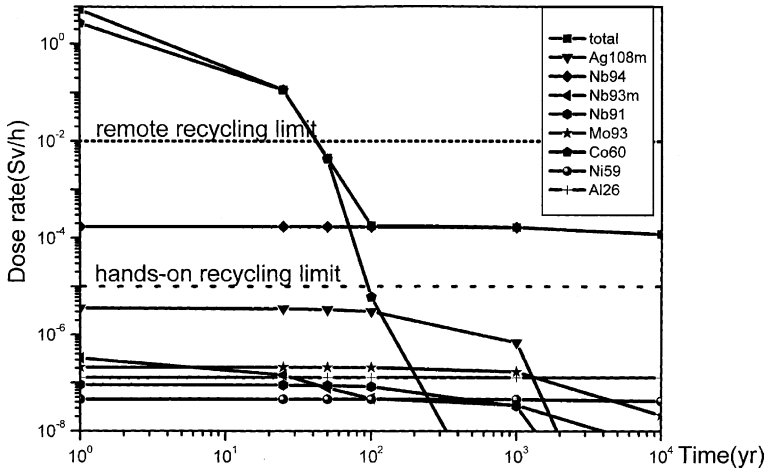

Fig. 5. Contribution of impurities to the dose rate of VH1 from the FBB model.

rate of the alloys at a cooling time of up to about 100 years, this comes from the reactions Co59(n,γ)Co60 and Co59(n,γ)Co60m(IT)Co60. After that time, the isotope Nb94 dominates the total dose rate, produced via the reactions Nb93(n,γ)Nb94m(IT)Nb94 and Nb93(n,γ)Nb94. The dose level contributed by Nb94 is lower than the remotely recycling limit. The isotope Ag108m has an important contribution to the long-term dose rate as well, this is produced via the reactions Ag107(n,γ)Ag108m and Ag109(n,2n)Ag108m. It is clear that the contact dose rates vs. time after irradiation have the similar trend for both the models.

More details including the required impurity control levels for remotely and hands-on recycling and the comparison of various vanadium alloy HEATs can be seen in Ref. [22].

3.3.2. Ferritic steel FS

The contact dose rates vs. time after irradiation for FS are shown in Figs. 6 and 7. It is noted that the isotope Co60 dominates the total dose rate at a cooling time of up to about 100 years and Fe55 gives some contribution to the dose rate during this period of time as well. These nuclides are produced via the reactions Fe58(n,γ)Fe59(β^-)Co59(n,γ)Co60, Fe56(n,2n)Fe55 and Fe54(n,γ)Fe55, respectively. After that time, Nb94 dominates the total dose rate, it is mainly produced via the reactions Mo94(n,p)Nb94, Mo95(n,d)Nb94, Nb93(n,γ)Nb94m(IT)Nb94 and Nb93(n,γ)Nb94, respectively. There is a slight increase in the dose rate of Nb93m in the period of 10^3 years because of the reaction Mo93(β^+)Nb93m. The dose rate of Nb94 is less than the remotely recycling limit.

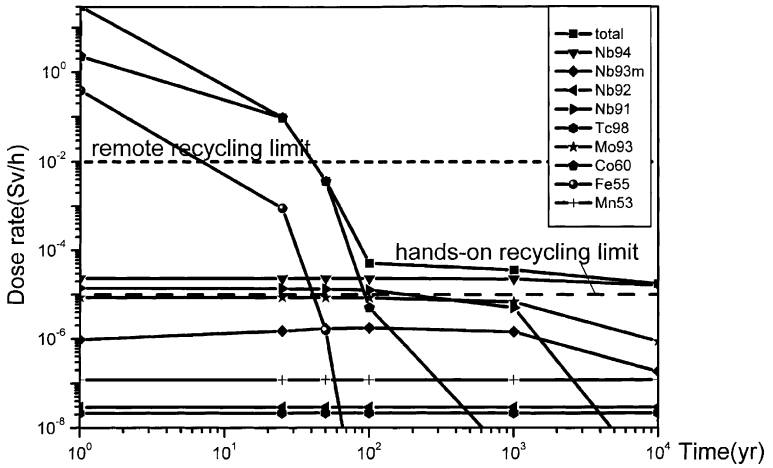

Fig. 6. Contribution of compositions to the dose rate of FS from the TBB model.

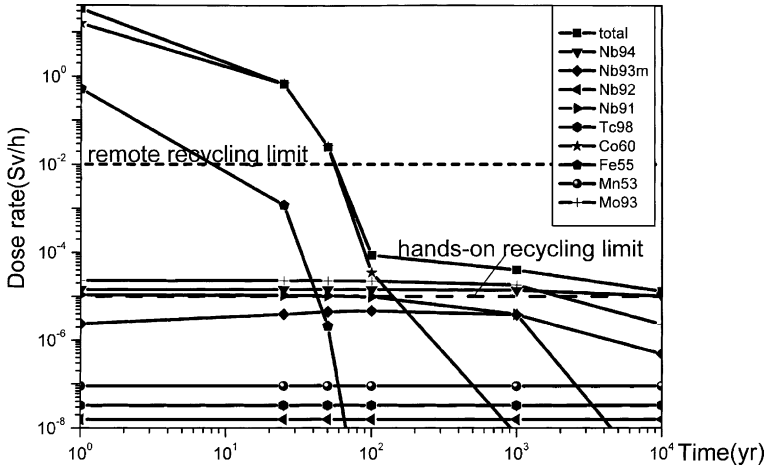

Fig. 7. Contribution of compositions to the dose rate of FS from the FBB model.

4. Conclusion

The activation characteristics of the three kinds of structural materials, i.e. 316L, ferritic steel and V-alloy, for the FDS-RT TBB model and FBB model are investigated and compared. The effect of factors such as the spectra, neutron fluence and strength, fusion and fission neutrons in the blanket on the activation characteristics of the structural materials are considered.

(1) The spectrum at the SW is very similar for each of the structural materials for the TBB or FBB model, and there are peaks at both low and high neutron energies. Higher fluxes for the FBB model are due to lower energy fission neutrons in the blanket. VH1 as the structural material has the highest flux compared with the other two SWs with the same model.
(2) Long-term dose closely depends on the neutron fluence. Short-term dose depends on the neutron source intensity, i.e. neutron wall loading P_w.
(3) The total dose rate for the FBB model is few times higher than that of the TBB model due to different spectra induced by hybrid neutrons in the FBB model.
(4) For vanadium alloy VH1, Co60 which originates from Co59 dominates the total dose rate at a cooling time of up to about 100 years. After that time, Nb94 which originates from Nb93 dominates the total dose rate. The dose rate level of Nb94 is lower than the remotely recycling limit. Ag108m has an important contribution to the long-term dose rate as well.

(5) For ferritic steel FS, Co60 which originates from Fe58 dominates the total dose rate at a cooling time of up to about 100 years and Fe55 gives some contribution to the dose rate during this period of time as well. After that time, Nb94 which originates from Mo94, Mo95 and Nb93 dominates the total dose rate. The dose rate of Nb94 is less than the remote-recycling limit. There is a slight increase in the dose rate of Nb93m in the period of 10^3 years because of the reaction Mo93(β^+)Nb93m.

Acknowledgement

This work is partly supported by Chinese National Natural Science Foundation with grant number 10175067.

References

[1] Y. Wu, Plasma Sci. Technol. 3 (6) (2001).
[2] Y. Chen, Y. Wu, Fusion Eng. Des. 49&50 (2000) 507.
[3] Y. Wu, L. Qiu, Y. Chen, Fusion Eng. Des. 51&52 (2000) 395.
[4] Y. Wu, International Symposium on Fusion Nuclear Technology, San Diego, USA, 7–13 April 2002.
[5] S. Zinkle, H. Matsui, D.L. Smith, A.F. Rowclifffe, E. van Osch, K. Abe, V.A. Kazakov, J. Nucl. Mater. 258–263 (1998) 205.
[6] D.L. Smith, H.M. Chung, H. Matsui, A.F. Rowclifffe, Fusion Eng. Des. 41 (1998) 7.
[7] H. Matsui, K. Fukumoto, D.L. Smith, H.M. Chung, W. van Witzenburg, S.N. Votinov, J. Nucl. Mater. 233–237 (1996) 92.
[8] W.R. Johnson, J.P. Smith, J. Nucl. Mater. 258–263 (1998) 1425.
[9] N.P. Taylor, C.B.A. Forty, J. Nucl. Mater. 283–287 (2000) 28.
[10] E.T. Cheng, T. Muroga, J. Nucl. Mater. 258–263 (1998).
[11] Y. Wu et al., these Proceedings.
[12] T.J. Dolan, G.J. Butterworth, Fusion Technol. 26 (1994) 1014.
[13] D.A. Petti, K.A. McCarthy, N.P. Taylor, C.B.A. Forty, R.A. Forrest, Fusion Eng. Des. 51&52 (2000) 435.
[14] T. Muroga, T. Nagasaka, A. Iiyoshi, A. Kawabata, S. Sakurai, M. Sakata, J. Nucl. Mater. 283–287 (2000) 711.
[15] T. Muroga, T. Nagasaka, Int. J. Refract. Met. Hard Mater. 225–230 (2000) 18.
[16] M. Merola, M. Zucchetti, Fusion Technol. 21 (1992).
[17] J.P. Qian, 5th International Symposium on Fusion Nuclear Technology (ISFNT-5), Rome, Italy, 19–24 September 1999.
[18] S. Zheng, Y. Wu, Q. Huang, Plasma Sci. Technol. 4 (2) (2002).
[19] S. Zheng, Y. Wu, Plasma Sci. Technol. 4 (2002) 1421.
[20] J.F. Briesmeister (Ed.), Transport Methods Group, Los Alamos National Laboratory, LA-12625-M, Version 4B, 1997.
[21] R.A. Forrest, J.-Ch. Sublet, UKAEA FUS 407, 1998.
[22] Y. Wu, T. Muroga, et al., these Proceedings.
[23] Y.P. Zeng, F.R. Wan, W.Y. Chu, J. Nucl. Mater. 228 (1996) 135.
[24] S. Nagatanigawa, Y. Miyama, Manual of Nuclear Reactor Materials, Z. Shouyi, Trans., Beijing Atomic Energy, 1987 (in Chinese).
[25] Q. Huang, Y. Wu, 6th Japan-China Symposium on Materials for Advanced Energy Systems and Fission & Fusion Engineering, Kyushu, Japan, 2000.